OPEN ACCESS

IOP Publishing | International Atomic Energy Agency

Nuclear Fusion

Nucl. Fusion **57** (2017) 056018 (14pp)

https://doi.org/10.1088/1741-4326/aa6355

Runaway electrons and ITER

Allen H. Boozer

Columbia University, New York, NY 10027, United States of America

E-mail: ahb17@columbia.edu

Received 1 September 2016, revised 29 January 2017
Accepted for publication 27 February 2017
Published 24 March 2017

Abstract

The potential for damage, the magnitude of the extrapolation, and the importance of the atypical—incidents that occur once in a thousand shots—make theory and simulation essential for ensuring that relativistic runaway electrons will not prevent ITER from achieving its mission. Most of the theoretical literature on electron runaway assumes magnetic surfaces exist. ITER planning for the avoidance of halo and runaway currents is focused on massive-gas or shattered-pellet injection of impurities. In simulations of experiments, such injections lead to a rapid large-scale magnetic-surface breakup. Surface breakup, which is a magnetic reconnection, can occur on a quasi-ideal Alfvénic time scale when the resistance is sufficiently small. Nevertheless, the removal of the bulk of the poloidal flux, as in halo-current mitigation, is on a resistive time scale. The acceleration of electrons to relativistic energies requires the confinement of some tubes of magnetic flux within the plasma and a resistive time scale. The interpretation of experiments on existing tokamaks and their extrapolation to ITER should carefully distinguish confined versus unconfined magnetic field lines and quasi-ideal versus resistive evolution. The separation of quasi-ideal from resistive evolution is extremely challenging numerically, but is greatly simplified by constraints of Maxwell's equations, and in particular those associated with magnetic helicity. The physics of electron runaway along confined magnetic field lines is clarified by relations among the poloidal flux change required for an e-fold in the number of electrons, the energy distribution of the relativistic electrons, and the number of relativistic electron strikes that can be expected in a single disruption event.

Keywords: runaway electrons, ITER, tokamaks, magnetic helicity, disruptions, fast magnetic reconnection

(Some figures may appear in colour only in the online journal)

1. Introduction

The danger to the ITER mission posed by runaway electrons became apparent two decades ago [1–3]. Research has been extensive; more than one hundred and fifty papers can be found searching on 'runaway electrons' and 'ITER'. Nevertheless, the implications of runaway electrons on achieving the ITER mission remain uncertain. As stated by Lehnen *et al* [4] in 2015: '*A suitable scheme for the active suppression or mitigation of runaway electrons has not yet been confirmed.*' Time pressures exist. As Lehnen *et al* [4] noted: '*A decision on the final design is scheduled to be taken in 2017.*'

The potential for damage, the magnitude of the extrapolation, and the importance of the atypical imply that theory and simulation—tested where possible by experiments—are required for high credibility that runaway electrons will not prevent ITER from achieving its mission. Major relativistic-electron incidents that require months to repair should be separated by years to avoid compromising the achievement of the ITER mission. This is of order once in a thousand shots.

In principle, a plan for the adequate protection of ITER cannot be validated on existing tokamaks—they are too small for a reliable extrapolation. A measure of the extrapolation was given in [3]: the avalanche process can multiply the number of relativistic electrons by about twelve orders of magnitude more in ITER than in JET. The importance of atypical events—once in a thousand shots—makes it impractical to have a low-risk

empirical demonstration by running a sufficient number of shots at each level of increasing plasma current.

The interpretation of experiments on existing tokamaks and their extrapolation to ITER requires two careful physics distinctions: confined versus unconfined magnetic field lines and quasi-ideal versus resistive evolution.

The classical theory of runaway electrons [1, 2] and most of the theoretical literature assume the magnetic field lines remain confined. Experiments and their simulation [5–8] imply that most field lines do not.

The most energy an electron can gain in one toroidal transit is the local loop voltage, V_ℓ. To avoid halo currents, the poloidal flux in an ITER plasma, $\sim 75\,\mathrm{V}\cdot\,\mathrm{s}$, may need to be removed on the resistive time scale of the walls, ~ 150 ms, which gives $V_\ell \sim 500$ V. When $V_\ell \sim 500$ V, electrons cannot runaway to relativistic energies when they are on magnetic field lines that make fewer that $\sim 10^3$ circuits before intercepting the walls. Nevertheless, when even a small fraction of the toroidal flux lies in flux tubes that do not intercept the walls, the breakup of magnetic surfaces can result in a strong relativistic current within the non-intercepting flux tubes: (1) Electrons moving within the non-intercepting flux tubes can make a sufficient number of toroidal transits to become highly relativistic. (2) As will be shown, a skin current naturally arises on the surface of a non-intercepting flux tube, which can produce a loop voltage far greater than 500 V.

The upward spike in the plasma current and the large drop in the internal inductance ℓ_i that occurs on a 1 ms time scale during thermal quenches are symptomatic of the breakup of magnetic surfaces by a fast magnetic reconnection. Even when the plasma resistivity is arbitrarily small, the breaking of magnetic surfaces can be fast and independent of the resistivity—of order tens to hundreds of toroidal transit times of an Alfvén wave—either due to to the formation of plasmoids as recently reviewed by Loureiro and Uzdensky [9] or as cited in [9] due to [10] the exponentially increasing separation of neighboring magnetic field lines figure 1.

The breaking of magnetic surfaces forces a flattening of the parallel current density $j_\parallel$ on a shear Alvén time scale. As will be shown in section 2, this leads to a drop in the plasma internal inductance and an upward spike in the plasma current. Magnetic field lines joined in a fast reconnection generically have distinct parallel current densities $j_\parallel$. The smallness of the Debye length implies the current density is divergence free in fusion plasmas [11], which can be written as $\vec{B}\cdot\vec{\nabla}(j_\parallel/B) = \vec{\nabla}\cdot(\vec{f}\times\vec{B}/B^2)$, where $\vec{f} = \vec{j}\times\vec{B}$ is the magnetic force on the plasma. There are two possible plasma forces: one due to the divergence of the plasma pressure tensor, which includes the viscous force, and the other inertial, $m_i n \mathrm{d}\vec{v}/\mathrm{d}t = \vec{f}$. Unless the plasma viscosity is sufficiently large, the inertial force is required, and $j_\parallel/B$ relaxes to an equilibrium value on the time scale for a shear Alfvén wave to propagate along the magnetic field lines and cover the region over which the reconnection occurred [10], $\partial^2(j_\parallel/B)/\partial t^2 = V_A^2\partial^2(j_\parallel/B)/\partial\ell^2$.

Although magnetic surfaces can be broken on a quasi-ideal, Alfvénic rather than resistive, time scale, a parallel electric field, such as that due to the plasma resistivity η, is required to accelerate electrons along magnetic flux tubes that do not intercept the chamber walls, section 2.3.1. The reconnection can greatly enhance $E_\parallel = \eta j_\parallel$ since it naturally produces a skin current on the surface of a non-intercepting flux tube.

A realistic simulation of the transfer of the plasma current from thermal to relativistic carriers must separate the quasi-ideal evolution of fast magnetic reconnection from the resistive evolution of electron acceleration. Unfortunately, the spatial resolution required to accurately simulate a surface-breaking quasi-ideal evolution during a current spike is sufficiently far beyond present computational capabilities that its accomplishment before ITER is completed is unclear. Nevertheless, numerical studies of simplified systems that undergo fast magnetic reconnection could clarify the physics of magnetic reconnection. Simulations could illuminate the subtle behavior of the shear Alfvén waves, which undergo strong damping in regions of stochastic magnetic field lines [10, 12], and the time development of magnetic reconnections in continuously evolving systems, such at the one illustrated in figure 1. Some time, called the trigger time, is required for the field lines to become sufficiently complicated to trigger a reconnection. Magnetic perturbations that resulted in a thermal quench in JET [13] were seen on a number of time scales, but a slow natural growth, ≈ 400 ms, could occur before the fast reconnection was triggered. Once reconnection begins, it causes a magnetic relaxation in one region. The restoration of force balance by Alfvén waves can add to the field line complexity in another region triggering additional reconnections. This Alfvénic effect defines the duration of a reconnection event, which appears to be of order 1 ms in large tokamaks. Nardon *et al* saw an avalanche of tearing modes during the initiation of a thermal quench in their JOREK simulations [8] even though the code was not run with the spatial resolution required for reconnection on an Alfvénic time scale.

Although it is unlikely that simulations of quasi-ideal reconnections can be used directly to determine the implications of current spikes on electron runaway, Maxwell's equations constrain what is possible in a quasi-ideal evolution. As will be shown, these constraints can be used to study the implications of experiments on existing tokamaks to electron runaway on ITER.

Studies of electron runaway in existing experiments require an understanding of (1) magnetic surface breakup and (2) the implications for electron acceleration due to the plasma resistivity within the remaining tubes of non-intercepting magnetic field lines. Consequently, this paper has two primary sections: section 2 derives the fundamental constraint that Maxwell's equations place on a quasi-ideal evolution, which is the evolution equation for magnetic helicity, $\int\vec{A}\cdot\vec{B}\mathrm{d}^3x$, and gives illustrative calculations. Section 3 gives results for quantities that circumscribe the runaway to relativistic energies of electrons that lie within non-intercepting flux tubes. Some of the results of section 3 are new, such as the multiple roles of the dimensionless quantity γ_{ef}, others place known results in a more transparent and useful form.

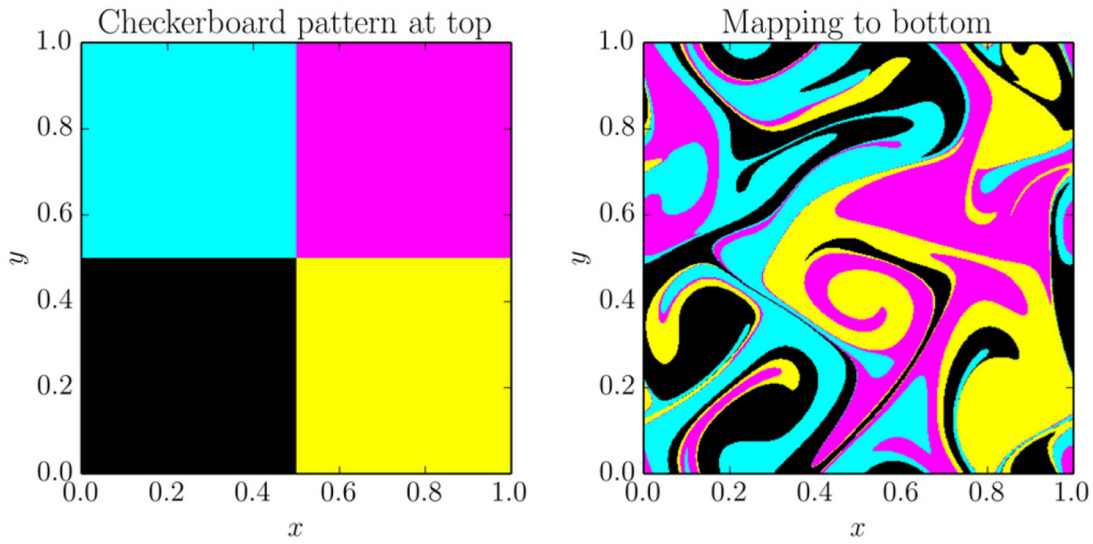

Figure 1. The physics that leads to fast magnetic reconnection in three dimensional systems can be modeled by a magnetic field embedded in a perfectly conducting plasma between two perfectly conducting constant-z planes in x, y, z Cartesian coordinates. Periodicity in x and y is assumed. The top constant-z plane is rigid while the bottom constant-z plane is a perfectly-conducting, flowing, incompressible fluid. Initially the magnetic field lines have only a $\hat{z}$ component. Because of the perfect conductivity assumptions, each field line has a fixed interception with the top plane but its interception with the bottom plane is transported by the fluid flow. The figure illustrates these transported interceptions with the bottom plane of field lines that lie in four squares in the top plane. Although the boundaries between the four regions cannot break, their distortions become ever greater—generally exponentially in time. Eventually non-ideal effects, such as electron inertia, which defines a spatial scale c/ω_{pe}, blur the boundaries and break the magnetic field line connections. Reproduced courtesy of IAEA. Figure from [11]. Copyright (2015) IAEA.

The appendix discusses plasma cooling, which is required to increase the plasma resistivity so the plasma current can be terminated sufficiently rapidly to avoid halo currents. When cooling is too rapid, electron runaway naturally occurs. It is shown that the speed of cooling required to avoid halo currents is significantly slower than that required to produce an electron runaway. This suggests that ITER plasmas could be terminated sufficiently rapidly to avoid halo currents without the danger of electron runaway by a carefully orchestrated cooling. However, the required level of control is probably beyond what can be achieved.

2. Magnetic surface breakup

2.1. Natural and forced surface breakup

The fast breakup of magnetic surfaces can arise as part of a natural plasma evolution [13] or be forced [14, 15]. A forced breakup often arises from efforts to mitigate halo currents and heat loads through the injection of impurities. The physics of thermal quenches, whether naturally occurring or produced by impurity injection, has much in common [14]. The breakup of surfaces and the associated rapid thermal quench due to massive-gas or shattered-pellet injection have been seen in a number of simulations [5–8].

The achievement of the ITER mission could be endangered by machine damage not only from relativistic electrons but also from halo currents [3]. Halo currents arise when axisymmetric position control is lost and plasma is scraped off by the walls faster than the plasma current decays [16]. This causes the edge safety factor q_e to drop on the resistive time scale of the walls, ~ 150 ms in ITER. When $q_e \approx 2$, an external kink grows at whatever speed is required to induce a current along the open magnetic field lines in the halo just outside the main plasma body. This halo current allows the maintenance of force balance and slows the growth of the kink to a resistive time scale. Were it not for dangers of runaway electrons from rapid cooling, halo currents could be reliably avoided on ITER using massive-gas or shattered-pellet injection of impurities to produce a current quench within the required time range [4]. When the current-quench time is too long, a halo current arises. When too short, excessive eddy currents occur in the surrounding structures.

When the plasma cooling is too rapid, the plasma current can be transferred from thermal to relativistic runaway electrons, which can arrest the decay of the plasma current. The result could be damage both from a halo current and from the runaway electrons thrown into the wall by a kink. A kink can push a plasma into the walls at locations where normal magnetic field $\vec{B} \cdot \hat{n}$ is non-zero on a time scale set by the growth of the kink—the resistivity of the wall is irrelevant. This is seen in the growth of the kink associated with a halo current [16]. The vertical field in a tokamak ensures that there are extensive wall locations at which $\vec{B} \cdot \hat{n} \neq 0$.

As will be shown in appendix A.1, the cooling time must be very short, $\lesssim 20$ ms at the standard ITER operating density $10^{20}\mathrm{m}^3$ to produce runaway electrons. Nevertheless, magnetic surface breakup produces an even more rapid cooling, appendix A.2. The thermal quench times seen after massive-gas or shattered-pellet injection in large tokamaks [14, 15] is ~ 1 ms.

2.2. Non-intercepting flux tubes

The breakup of the magnetic surfaces would not pose a danger for acceleration of electrons to relativistic energies were it not for non-intercepting flux tubes, which contain magnetic field lines that do not intercept the walls. Non-intercepting flux tubes are seen in numerical simulations [5–8] of massive gas and shattered pellet injection—particularly near the magnetic axis and sometimes in the cores of magnetic islands. Non-intercepting flux tubes are also seen in models of the effects of non-axisymmetric magnetic fields [17, 18] and are found to provide excellent confinement of relativistic electrons [17, 19]. Unless the non-intercepting flux tubes dissipate before outer confining magnetic surfaces re-form, a highly dangerous situation arises. Electrons that were trapped and accelerated in these flux tubes can fill a large volume of stochastic field lines and serve as a seed for the transfer of the full plasma current to runaways. When the outer confining surfaces are later punctured, as by a drift into the wall, then the full runaway inventory will be lost in a short pulse along a narrow flux tube [20].

The reversion of the magnetic field lines to a simple state after a magnetic reconnection—such as re-formed magnetic surfaces—has been studied far less than the magnetic reconnection process itself. Since the work of Taylor [21], it has been known that an axisymmetric state can be the minimum energy state following a large scale breaking of surfaces and, therefore, a natural direction for the plasma evolution. The complete evolution is resistive because in its final state the magnetic field lines do not have the exponentially separating trajectories that make small non-ideal effects, such as c/ω_{pe}, important. If the flow in the bottom plane of figure 1 is stopped following a long period in which the flow was driving fast magnetic reconnection, then on a global resistive time scale the magnetic field lines will revert to having only a uniform $\hat{z}$ component. Without the energy input from the flow in the bottom plane, the plasma resistivity dissipates the plasma current density to zero.

Although not part of ITER planning, currents induced in the walls by the fast magnetic relaxation could be used to passively prevent outer surfaces from re-forming [22, 23].

When only a small tube of magnetic flux tube fails to intercept the walls, a large fraction of the entire plasma current can be transferred to that tube; see table 1. The tube presumably becomes kink unstable as its safety factor drops, which would transfer the relativistic electron current to the walls. But, the relativistic current transferred to the wall would be small when the toroidal flux in the tube, $\delta\psi_t$, is small compared to that in the plasma, $\Psi_t \approx 120\,\mathrm{V}\cdot\mathrm{s}$ for ITER. The current I in a flux tube with a safety factor q scales as $I \propto \delta\psi_t/q$.

2.3. Magnetic helicity constraint

When magnetic surfaces breakup on a short time scale compared to both the time scale for the quench of the plasma current, $\gtrsim 50$ ms, and the resistive time scale of the walls, ~ 150 ms in ITER, the magnetic helicity $K \equiv \int \vec{A}\cdot\vec{B}\mathrm{d}^3x$ in the region enclosed by the walls is conserved. Although the concept of magnetic helicity is known from Woltjer's 1958 paper [24] and the more than a thousand papers that followed on its applications to almost all areas of plasma physics, the implications for fast thermal quenches, ~ 1 ms, have not been appreciated. Even the applicability of helicity conservation to tokamaks is sometimes doubted, so both the derivation and implications will be discussed.

Table 1. The effect of a magnetic relaxation over the region $1 > s > s_r$ for an initial $\varpi = 2$ equilibrium is given for various s_r. The table gives the current spike $I_p^{(a)}/I_p^{(b)}$, the total plasma current after to that before the relaxation; the singular current $I_{sing}^{(a)}/I_p^{(b)}$ on the $s = s_r$ surface; and the rotational transform just outside the $s = s_r$ surface divided by the central rotational transform.

s_r	$\frac{I_p^{(a)}}{I_p^{(b)}}$	$\frac{I_{sing}^{(a)}}{I_p^{(b)}}$	$\frac{\iota_a(s_r+)}{\iota(0)}$
0.1	1.1916	0.7837	1.342
0.2	1.1394	0.3696	1.085
0.4	1.0708	0.1229	0.861
0.6	1.0294	0.0399	0.720
0.8	1.0070	0.0080	0.604
0.9	1.0017	0.0018	0.551

2.3.1. Constraint of Maxwell's equations on poloidal flux and magnetic helicity evolution. Any vector, including the vector potential, can be expanded in the form [11]

$$\vec{A} = \psi_t\vec{\nabla}\frac{\theta}{2\pi} - \psi_p\vec{\nabla}\frac{\varphi}{2\pi} + \vec{\nabla}g, \tag{1}$$

where θ and φ are poloidal and toroidal angles of a system of coordinates, figure 2. There is a freedom of gauge in the vector potential, which can be used to make $g = 0$. Taking the curl of the vector potential,

$$\vec{B} = \vec{\nabla}\psi_t\times\vec{\nabla}\frac{\theta}{2\pi} + \vec{\nabla}\frac{\varphi}{2\pi}\times\vec{\nabla}\psi_p; \tag{2}$$

$$\vec{A}\cdot\vec{B} = \left(\frac{\partial(\psi_p\psi_t)}{\partial\psi_t} - 2\psi_p\right)\frac{(\vec{\nabla}\psi_t\times\vec{\nabla}\theta)\cdot\vec{\nabla}\varphi}{(2\pi)^2}. \tag{3}$$

Canonical coordinates, figure 2 means points in space are specified by $\vec{x}(\psi_t,\theta,\varphi,t)$. When ψ_p is given as a function of (ψ_t,θ,φ), it is the Hamiltonian of the magnetic field lines. Field line topology and hence reconnection are determined by $\psi_p(\psi_t,\theta,\varphi,t)$. When a coordinate system $\vec{x}(\psi_t,\theta,\varphi,t)$ exists such that ψ_p has no explicit time dependence, the evolution is ideal, with no reconnection, and can proceed at a speed limited only by inertia or the speed of light, which means limited only by the speed of Alfvén waves. The poloidal flux outside a constant ψ_p surface is $\oint\vec{A}\cdot(\partial\vec{x}/\partial\varphi)\mathrm{d}\varphi = -\psi_p$. The toroidal flux inside a constant ψ_t surface is $\oint\vec{A}\cdot(\partial\vec{x}/\partial\theta)\mathrm{d}\theta = \psi_t$. More details on the derivations given in this paragraph can be found in [11]. The freedom of the coordinate system $\vec{x}(\psi_t,\theta,\varphi,t)$ can be used to efficiently represent magnetic relaxations in axisymmetric tokamaks.

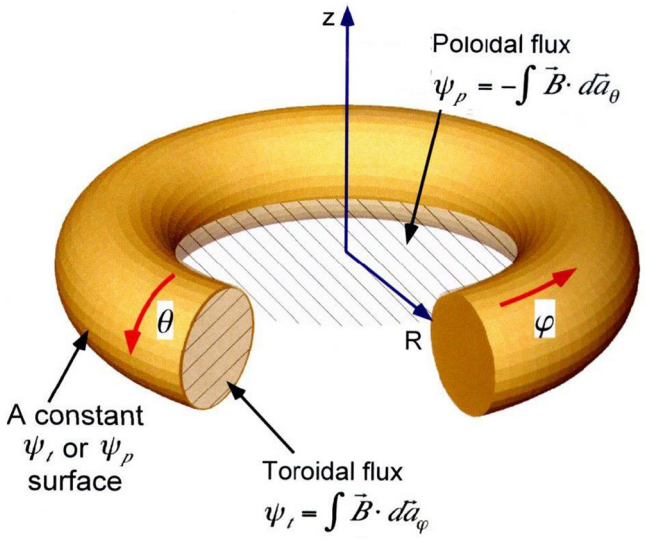

Figure 2. The relationship is given between (R, φ, Z) cylindrical coordinates and $(\psi_t, \theta, \varphi)$ canonical coordinates of the magnetic field as well as the meaning of the poloidal $\psi_{\rm p}$ and toroidal ψ_t magnetic fluxes.

The helicity content of a region enclosed by a surface of constant toroidal flux Ψ_t will be defined as

$$K_c(\Psi_t, t) \equiv \int \vec{A}\cdot\vec{B}\mathrm{d}^3x - \bar{\psi}_{\rm p}(\Psi_t, t)\Psi_t, \text{ so} \tag{4}$$

$$= -2\int_0^{\Psi_t} \bar{\psi}_{\rm p}\mathrm{d}\psi_t, \text{ where} \tag{5}$$

$$\bar{\psi}_{\rm p}(\psi_t, t) \equiv \oint \psi_{\rm p}(\psi_t, \theta, \varphi, t)\frac{\mathrm{d}\theta\mathrm{d}\varphi}{(2\pi)^2}. \tag{6}$$

The helicity content K_c yields somewhat simpler equations than the helicity itself, $K \equiv \int \vec{A}\cdot\vec{B}\mathrm{d}^3x$, in part by the removal of the arbitrariness of gauge by the choice $g = 0$ in equation (1). The important features of the helicity content are its simple relation to the poloidal and toroidal fluxes, equation (5), and its evolution, equation (14), which has the general validity of Faraday's Law.

Faraday's law implies the electric field has the form $\vec{E} = -(\partial\vec{A}/\partial t)_{\vec{x}} - \vec{\nabla}\Phi$. The appendix to [11] derives the identity

$$\left(\frac{\partial\vec{A}}{\partial t}\right)_{\vec{x}} = -\left(\frac{\partial\psi_{\rm p}}{\partial t}\right)_c \vec{\nabla}\frac{\varphi}{2\pi} + \vec{u}_c\times\vec{B} - \vec{\nabla}(\vec{u}_c\cdot\vec{A}), \tag{7}$$

where $\vec{u}_c \equiv \partial\vec{x}(\psi_t, \theta, \varphi, t)/\partial t$ is the velocity of the canonical coordinates through space. The subscript c implies the canonical coordinates are held fixed. Consequently, the electric field always has the form

$$\vec{E} + \vec{u}_c\times\vec{B} = \left(\frac{\partial\psi_{\rm p}}{\partial t}\right)_c \vec{\nabla}\frac{\varphi}{2\pi} - \vec{\nabla}\Phi_c, \tag{8}$$

where $\Phi_c \equiv \Phi - \vec{u}_c\cdot\vec{A}$.

Since $\vec{B}\cdot\vec{\nabla}\varphi/2\pi = 1/(2\pi)^2\mathcal{J}$, where $\mathcal{J}$ is the Jacobian of canonical coordinates, equation (8) for the electric field gives an evolution equation for the poloidal flux averaged over a surface of constant toroidal flux, equation (6), which is

$$\frac{\partial\bar{\psi}_{\rm p}}{\partial t} = \bar{V}_\ell - \frac{\partial}{\partial\psi_t}\mathcal{F}_\parallel; \tag{9}$$

$$\bar{V}_\ell(\psi_t, t) \equiv \oint \vec{E}\cdot\vec{B}\mathcal{J}\mathrm{d}\theta\mathrm{d}\varphi; \tag{10}$$

$$\mathcal{F}_\parallel(\psi_t, t) = -\oint \Phi_c\vec{B}\cdot\vec{\nabla}\psi_t\mathcal{J}\mathrm{d}\theta\mathrm{d}\varphi. \tag{11}$$

$\bar{V}_\ell$ is a loop voltage. Note that even when $\bar{V}_\ell = 0$ the magnetic topology, which is determined by $\psi_{\rm p}(\psi_t, \theta, \varphi, t)$, can change.

The flux of $\bar{\psi}_{\rm p}$ due to its flow along magnetic field lines is given by $\mathcal{F}_\parallel$. When the potential Φ_c has no θ variation, $\mathcal{F}_\parallel = 0$ because $\mathcal{J}\vec{B}\cdot\vec{\nabla}\psi_t \propto \partial\psi_{\rm p}/\partial\theta$ and $\psi_{\rm p}$ must be a periodic function of θ. The variation in the potential Φ_c in a ψ_t surface that can contribute to $\mathcal{F}_\parallel$ is given by

$$\frac{\partial\Phi_c}{\partial\theta} = -\left(\vec{E}\cdot\frac{\partial\vec{x}}{\partial\theta} + \frac{\vec{u}_c\cdot\vec{\nabla}\psi_t}{2\pi} + \frac{\vec{u}_c\cdot\vec{\nabla}\varphi}{2\pi}\frac{\partial\psi_{\rm p}}{\partial\theta}\right). \tag{12}$$

The parallel flux of the poloidal magnetic flux is

$$\mathcal{F}_\parallel = \oint\psi_{\rm p}\left(\vec{E}\cdot\frac{\partial\vec{x}}{\partial\theta} + \frac{\vec{u}_c\cdot\vec{\nabla}\psi_t}{2\pi} + \frac{\vec{u}_c\cdot\vec{\nabla}\varphi}{2\pi}\frac{\partial\psi_{\rm p}}{\partial\theta}\right)\frac{\mathrm{d}\theta\mathrm{d}\varphi}{2\pi}. \tag{13}$$

The parallel-transport $\mathcal{F}_\parallel$ vanishes when either the ψ_t surfaces are magnetic surfaces or when $\vec{u}_c = 0$ in a perfect conductor, which is defined by $\vec{E} = 0$.

The first term on the right hand side of equation (13) is of importance in electrostatic helicity injection. Helicity is injected when the electrostatic potential changes across a slot in the walls through which magnetic field lines either enter or leave the plasma chamber. The terms involving $\vec{u}_c \equiv \partial\vec{x}(\psi_t, \theta, \varphi, t)/\partial t$ on the right hand side of equation (13) arise due to the changing reference frame when $\vec{u}_c$ is non-zero. When the walls are fixed and sufficiently highly conducting that negligible toroidal flux slips through, one can choose $\vec{u}_c$ to be zero there.

The evolution of the helicity content is given by

$$\frac{\mathrm{d}K_c}{\mathrm{d}t} = -2\int_0^{\Psi_t}\frac{\partial\bar{\psi}_{\rm p}}{\partial t}\mathrm{d}\psi_t = -2\int\vec{E}\cdot\vec{B}\mathrm{d}^3x + 2\mathcal{F}_\parallel(\Psi_t, t). \tag{14}$$

The helicity content of a constant Ψ_t surface is changed only by the volumetric term $\int\vec{E}\cdot\vec{B}\mathrm{d}^3x$ and by the flux $2\mathcal{F}_\parallel(\Psi_t, t)$ of helicity through the boundary.

In a quasi-ideal evolution in a region of space, the magnetic helicity content K_c of that region is conserved; $\mathrm{d}K_c/\mathrm{d}t = -2\int\bar{V}_\ell\mathrm{d}\psi_t = 0$ This has the important implication that the average loop voltage is zero, so an electron that stochastically covers the region has no net acceleration.

2.3.2. Implications of Ohm's law. Equation (14) for the evolution of the helicity content has the general validity of Maxwell's equations. Going beyond Maxwell's equations by the use of the parallel Ohm's law, $\vec{E}\cdot\vec{B}=\eta\vec{j}\cdot\vec{B}$, gives an expression for the evolution of the helicity content as a product of a global plasma resistance $\bar{\mathcal{R}}$, the net plasma current $I_{\rm p}$, and the toroidal flux Ψ_t in the plasma chamber:

$$\int\vec{E}\cdot\vec{B}\,\mathrm{d}^3x=\bar{\mathcal{R}}I_{\rm p}\Psi_t; \tag{15}$$

$$\begin{aligned} I_{\rm p}&\equiv\int\vec{j}\cdot\vec{\nabla}\frac{\varphi}{2\pi}\mathrm{d}^3x\\ &=\int_0^{\Psi_t}\frac{j_\parallel}{B}\mathrm{d}\psi_t\frac{\mathrm{d}\theta\mathrm{d}\varphi}{(2\pi)^2}; \end{aligned} \tag{16}$$

$$\begin{aligned} \bar{\mathcal{R}}&\equiv\frac{\int(2\pi R_B\eta B)\frac{j_\parallel}{B}\mathrm{d}\psi_t\frac{\mathrm{d}\theta\mathrm{d}\varphi}{(2\pi)^2}}{I_{\rm p}\Psi_t}\\ &=\frac{\langle 2\pi R_B\eta B\rangle_{j_\parallel/B}}{\Psi_t}, \end{aligned} \tag{17}$$

where the effective local major radius is $R_B\equiv B/\vec{B}\cdot\vec{\nabla}\varphi$.

The loop voltage $\bar{V}_\ell$, defined in equation 10 can be written as

$$\bar{V}_\ell=\mathcal{R}_\psi\frac{\partial I}{\partial\psi_t}; \tag{18}$$

$$I(\psi_t,t)=\int_0^{\psi_t}\frac{j_\parallel}{B}\mathrm{d}\psi_t\frac{\mathrm{d}\theta\mathrm{d}\varphi}{(2\pi)^2}; \tag{19}$$

$$\mathcal{R}_\psi\equiv\frac{\oint(2\pi R_B\eta B)\frac{j_\parallel}{B}\frac{\mathrm{d}\theta\mathrm{d}\varphi}{(2\pi)^2}}{\oint\frac{j_\parallel}{B}\frac{\mathrm{d}\theta\mathrm{d}\varphi}{(2\pi)^2}}, \tag{20}$$

so $I_{\rm p}(t)=I(\Psi_t,t)$, and $\partial I/\partial\psi_t=\langle j_\parallel/B\rangle$ is a $\theta-\varphi$ average of $j_\parallel/B$.

The helicity content is related to the net plasma current and the total toroidal flux by an inductance $K_c=2L_kI_{\rm p}\Psi_{\rm p}$, where $L_k\sim\mu_0R_0$, section 2.4. When the magnetic evolution is rapid compared to the $L_k/\bar{\mathcal{R}}$ time, the helicity content is conserved. When the chamber walls do not fit tightly around the plasma, the global resistance $\bar{\mathcal{R}}$ can be enhanced by the halo currents that flow in the resistive halo plasma [16].

When the profile of the flux is fixed, which means $\bar{\psi}_{\rm p}(\psi_t,t)$ is the product of a function of toroidal flux and a function of time, the $L_k/\bar{\mathcal{R}}$ time is also the decay time for the poloidal magnetic flux, and $\bar{\mathcal{R}}$ can be thought of as the resistance of the tokamak plasma. During a fast magnetic relaxation, magnetic field lines associated with different $\bar{\psi}_{\rm p}$ are joined, which allows $\bar{\psi}_{\rm p}(\psi_t)$ to change as rapidly as the reconnection takes place though the decay time of the helicity content remains $L_k/\bar{\mathcal{R}}$. An implication is that the bulk of the poloidal flux and the net plasma current can never be removed from a plasma faster than on the $L_k/\bar{\mathcal{R}}$ time scale, which is a strong constraint on the mitigation of halo currents.

2.4. Tokamak equilibria

The information on axisymmetric plasma equilibria that is essential for studying the effects of magnetic surface breakup on the phenomenon of electron runaway can be simply obtained. The poloidal flux and poloidal field energy as well as the helicity are largely determined by the dependence of the enclosed plasma current $I(s)$ on $s\equiv\psi_t/\Psi_t$, where ψ_t is the toroidal flux enclosed by a magnetic surface and Ψ_t is the toroidal flux enclosed by the plasma chamber.

The enclosed plasma current, equation (19), will be modeled as

$$I(s)=I_{\rm p}(1-(1-s)^{\varpi}), \tag{21}$$

where $I_{\rm p}$ is the total plasma current given by equation (16). The current profile parameter is ϖ, which is a variant form of the Greek letter π. The current density, which is given by $\langle j_\parallel/B\rangle=(\mathrm{d}I/\mathrm{d}s)/\Psi_t=\varpi(1-s)^{\varpi-1}I_{\rm p}/\Psi_t$, is positive everywhere.

When the shapes of the magnetic surfaces are known, $\vec{x}(s,\theta,\varphi)$, an exact expression for the rotational transform $\iota(s)=1/q$ is given by equation (237) of reference [11]. In axisymmetry, the rotational transform can be written as

$$\iota(s)=\frac{L(s)I(s)}{2s\Psi_t},\ \text{where} \tag{22}$$

$$L(s)=\gamma(s)\mu_0R_0, \tag{23}$$

and $\gamma(s)$ is a dimensionless function essentially determined by the shapes of the surfaces. Equation (22) for the rotational transform is made plausible by the cylindrical expression, $\iota(r)=(R_0/r)B_\theta/B_z$ where the poloidal field $B_\theta=\mu_0I(r)/2\pi r$ and $2\pi R_0$ is the assumed periodicity distance along the z axis. The toroidal flux is $\psi_t=B_z\pi r^2$, so in a cylinder $\iota(s)=\mu_0R_0I(s)/2s\Psi_t$ with the shape parameter $\gamma(s)=1$.

An approximate expression can be derived for the surface-shape parameter $\gamma(s)$. Sufficiently close to the magnetic axis, analyticity requires that the surfaces have the shape $\vec{x}(s,\theta,\varphi)=(R_0+r\cos\theta)\hat{R}(\varphi)-\kappa_0r\sin\theta\hat{Z}$, where $\hat{R}$ and $\hat{Z}$ are the basis vectors of R,φ,Z cylindrical coordinates. The enclosed toroidal flux is $\psi_t=\pi\kappa_0r^2B_0$, where the magnetic field at the magnetic axis $B_0=\mu_0G/2\pi R_0$ with G the poloidal current enclosed by the magnetic axis. The implication is that $\gamma(s\to0)=2\kappa_0/(1+\kappa_0^2)$. Equation (21) for $I(s)$ implies the rotational transform at the magnetic axis is

$$\iota(0)=\frac{\varpi}{2}\frac{L_0}{\Psi_t}I_{\rm p},\ \text{where} \tag{24}$$

$$L_0\equiv L(0)=\frac{2\kappa_0}{1+\kappa_0^2}\mu_0R_0\approx6.61\frac{\mathrm{V\cdot s}}{\mathrm{MA}}. \tag{25}$$

The inductance L_0 was calculated assuming $\kappa_0=1.8$ and that the major radius $R_0=6.2$ m, both typical values for ITER. The toroidal flux in ITER is

$$\Psi_t=(5.3\ \mathrm{T})(22\ \mathrm{m}^2)\approx120\ \mathrm{V\cdot s}. \tag{26}$$

For the $I_p = 15$ MA ITER scenario, the central rotational transform is approximately unity, and equation (24) implies $\varpi \approx 2.5$. For simplicity, the geometric function $\gamma(s)$ will be assumed to be a constant, $\gamma(s) = \gamma(0)$, which gives $\iota(0)/\iota(1) = q_e/q_0 = \varpi$. The typical edge safety factor of ITER q_e is $q_{95} \approx 3$, which is 20% larger due to increased shaping near the edge, which reduces γ. The effects on integrals involving $\iota(s)$ over s would be expected to be smaller.

When ϖ is a low order integer, $\iota(s)$ can be written as an explicit polynomial, which can be integrated to obtain the poloidal flux as a polynomial since $\mathrm{d}\psi_p(s)/\mathrm{d}s = \iota(s)\Psi_t$. The poloidal flux at $s = 1$ will be taken to be zero:

$$\psi_p = (s-1)\Psi_p \text{ when } \varpi = 1 \tag{27}$$

$$= \frac{4s - s^2 - 3}{3}\Psi_p \text{ when } \varpi = 2 \tag{28}$$

$$= \frac{18s - 9s^2 + 2s^3 - 11}{11}\Psi_p \text{ when } \varpi = 3. \tag{29}$$

Since $-\psi_p$ is the poloidal flux outside a constant ψ_p surface, Ψ_p is the poloidal flux enclosed by the magnetic axis.

The flux inductance of the plasma can be determined using $\iota(0)\Psi_t = (\mathrm{d}\psi_p/\mathrm{d}s)_0$ with $\iota(0) = \varpi L_0 I_p/2\Psi_t$.

$$L_\psi \equiv \frac{\Psi_p}{I_p} = \frac{\varpi L_0}{\frac{2}{\Psi_p}\left(\frac{\mathrm{d}\psi_p}{\mathrm{d}s}\right)_0} \tag{30}$$

$$= \lambda_\psi(\varpi) L_0. \tag{31}$$

Three analytic results for $\lambda_\psi(\varpi)$ are $\lambda_\psi(1) = 1/2$, $\lambda_\psi(2) = 3/4$, and $\lambda_\psi(3) = 11/12$. These values are almost linearly dependent on ϖ, so other values such as $\lambda_\psi(2.5) \approx 0.83$ can be obtained by interpolation. The poloidal flux in ITER when $I_p = 15$ MA and $\varpi = 2.5$ is

$$\Psi_p \approx 82 \text{ V} \cdot \text{ s}. \tag{32}$$

Increased shaping, which makes $\gamma(s)$ smaller, reduces the flux inductance. In an ideal magnetic evolution, poloidal flux is conserved, so increased shaping increases the plasma current.

The plasma current and the magnetic helicity content are related by the helicity inductance,

$$L_k \equiv \frac{K_c}{2I_p\Psi_t} \tag{33}$$

$$= \lambda_k(\varpi) L_0. \tag{34}$$

Analytic expressions for $\lambda_k(\varpi)$ are $\lambda_k(1) = 1/2$, $\lambda_k(2) = 2/3$, and $\lambda_k(3) = 3/4$.

The poloidal magnetic field $\vec{B}_p$ in an axisymmetric equilibrium is defined by the $\vec{\nabla}(\varphi/2\pi) \times \vec{\nabla}\psi_p$ term in the contravariant representation of $\vec{B}$, equation (2). The general covariant representation [11] of the magnetic field is $\vec{B} = \mu_0 G(\psi_t)\vec{\nabla}(\varphi/2\pi) + \mu_0 I(\psi_t)\vec{\nabla}(\theta/2\pi) + \beta_*\vec{\nabla}\psi_t$, where G is the poloidal current outside and I is the toroidal current enclosed by a ψ_t surface. The poloidal field energy W_p is the volume integral of $\vec{B}_p \cdot \vec{B}/2\mu_0$, so

$$W_p = \frac{\Psi_t}{2}\int_0^1 I(s)\iota(s)\mathrm{d}s \tag{35}$$

$$= \frac{1}{4}\int_0^1 L(s)\frac{I^2(s)}{s}\mathrm{d}s \tag{36}$$

$$\approx \frac{L_0}{4}\ell_p I_p^2, \text{ where} \tag{37}$$

$$\ell_i \approx \frac{2\kappa_0}{1+\kappa_0^2}\ell_p. \tag{38}$$

That is internal inductance ℓ_i is the shape parameter times the internal inductance determined by the current profile ℓ_p. Analytic expressions for $\ell_p(\varpi)$ are $\ell_p(1) = 1/2$, $\ell_p(2) = 11/12$, and $\ell_p(3) = 73/60$. Interpolating to obtain $\ell_p(2.5) \approx 1.07$, the poloidal field energy when $I_p = 15$ MA, $\kappa_0 = 1.8$ and $\varpi = 2.5$ is

$$W_p = 396 \text{ MJ}; \tag{39}$$

the answer given in [3] is 395 MJ.

The poloidal field energy can also be written as $W_p = (\ell_p/\lambda_\psi)I_p\Psi_p$ where $\ell_p/\lambda_\psi = 1$ for $\varpi = 1, 11/9 \approx 1.222$ for $\varpi = 2$, and $11/9 \approx 1.327$ for $\varpi = 3$. A rough approximation is that $W_p \approx 0.3 I_p\Psi_p$.

2.5. Helicity conserving magnetic relaxations

A fast breakup of the magnetic surfaces flattens the $j_\parallel/B$ profile conserving the helicity and the poloidal flux ψ_p at $s = 1$, which is taken to be zero. When $j_\parallel/B$ is flattened over the entire plasma, the current profile parameter is $\varpi = 1$.

As an example of the effect of flattening, the effect of a rapid flattening from $\varpi = 3$ to $\varpi = 1$ will be calculated. The analytic answers for $K_c/(2I_p\Psi_t)$ for $\varpi = 1$ and 3 imply that the ratio of the plasma current after to that before the flattening is $I_p^{(a)}/I_p^{(b)} = 3/2$. The analytic expressions for Ψ_p/I_p for $\varpi = 1$ and 3, imply that the poloidal flux after minus the poloidal flux before the flattening is $\delta\bar{\psi}_p(s) = \{2 - 9s(1-s) - 2s^3\}\Psi_p^{(b)}/11$, where $\Psi_p^{(b)}$ is the poloidal flux enclosed by the axis before the reconnection. At the center $s = 0$, the poloidal flux increases from its pre-flattening negative value relative to the wall with $\delta\bar{\psi}_p(0) = 2\Psi_p^{(b)}/11$. The flux change for $s > 0.314$ is negative and reaches its maximum negative value at $s \approx 0.634$. The effect of rapid flux changes on driving runaway currents in any remaining magnetic islands was discussed in [19]. As shown by Woltjer [24], the magnetic field energy is reduced in a helicity conserving relaxation, but the reduction of the poloidal field energy is small, $W_p(\varpi = 1)/W_p(\varpi = 3) \approx 0.925$.

2.6. Breaking of outer surfaces

In simulations of thermal quenches and current spikes [5–8], tubes of magnetic flux that do not intercept the walls persist within the plasma volume. A more realistic model of what happens during a current spike may be to have the outer

magnetic surfaces break, $s > s_r$, while interior surfaces $s < s_r$ are preserved. In this model, the plasma current profile $I(s)$ remains unchanged during the spike for $s < s_r$ but the current density or equivalently dI/ds becomes independent of s for $s > s_r$. This model can be solved analytically when the initial profile coefficient ϖ is an integer. The simplest non-trivial case is $\varpi = 2$, the case that will be studied.

The helicity content of the annular region $s_r < s < 1$, before the relaxation was

$$K_{an}(s_r) = -2\Psi_t \int_{s_r}^{1} \psi_p(s) ds; \tag{40}$$

$$\frac{K_{an}(s_r)}{\Psi_p \Psi_t} = \frac{2}{9}(4 - s_r(3 - s_r)^2). \tag{41}$$

After the relaxation to $j_\parallel/B$ constant in the annulus $s > s_r$, the rotational transform has the form in that annulus

$$\iota_{(a)} = \left(\frac{c_1}{s} + c_2\right)\frac{\Psi_p}{\Psi_t} \text{ so} \tag{42}$$

$$\frac{\psi_p^{(a)}}{\Psi_p} = \frac{\psi_p(s_r)}{\Psi_p} + c_1 \ln\left(\frac{s}{s_r}\right) + c_2(s - s_r). \tag{43}$$

The constraints that set the two constants are $\psi_p^{(a)}(s = 1) = 0$ and the equality of K_{an} before and after the magnetic relaxation. There is a surface current at s_r given by the jump in ι there and a change in the plasma current I_p given by the change in ι at the edge $s = 1$. The two constants are given by

$$c_1 = \frac{K_{an} + \frac{\psi_p(s_r)}{\Psi_p}(1 - s_r)}{(1 + s_r)\ln s_r + 2(1 - s_r)}; \tag{44}$$

$$c_2 = \frac{-\frac{\psi_p(s_r)}{\Psi_p} + c_1 \ln s_r}{1 - s_r}. \tag{45}$$

The effect of the relaxation is given in table 1. As the poloidal flux associated with the surface current at s_r penetrates the confined region, it can drive an electron runaway. When s_r is small the rotational transform just outside the $s = s_r$ surface can become sufficiently large to drive a kink, which probably destroys the confined region. The rotational transform at the edge of a central flux tube, which contains toroidal flux $\delta\psi_t$ and encloses a toroidal current I is

$$\iota \propto \frac{I}{\delta\psi_t}. \tag{46}$$

When a flattened annulus is bounded by an outer region of magnetic surfaces as well an inner region, the value of the poloidal flux on the outer boundary of the annulus is to be chosen so it equals its pre-flattened value, which results in a surface current flowing on that boundary. The rotational transform at the plasma edge cannot change faster than the resistive time scale of the outer region of confining magnetic surfaces, so there is no spike in I_p.

3. Electron runaway along confined magnetic field lines

The classical theory of runaway electrons in ITER [1, 2] and much of the theoretical literature since has presumed that magnetic field lines remain well confined in the plasma volume. Following the current spike that accompanies a fast thermal quench, magnetic field lines that carry most of the toroidal magnetic flux in the plasma volume appear to intercept the walls. Only electrons that lie within tubes of magnetic flux that do not intercept the walls can runaway to relativistic energies, and in these tubes the classical theory applies. Simulations imply that after a thermal quench magnetic surfaces re-form, and the electrons that reached high energies within the non-intercepting flux tubes serve as seed electrons for the transfer of remaining plasma current from near-thermal to relativistic carriers. This can occur due to energetic electrons escaping from the non-intercepting flux tubes into the plasma region bounded by an outermost re-formed magnetic surface due to resistive dissipation of the non-intercepting tube or due to the tube becoming unstable as it picks up an ever larger fraction of the plasma current.

The theory of runaway electrons on confined magnetic field lines [25] is circumscribed by: (1) the number of energetic electrons remaining after a thermal quench, (2) the kinetic energy K_r required by an electron to runaway, and (3) the change in the poloidal flux $\gamma_{ef}\psi_{pa}$ required for an e-fold in the number of energetic electrons. Theory and simulations can obtain values for the last two quantities [25, 26] assuming no strong, short wavelength, magnetic turbulence is present. Known theory could be used to simulate existing experiments [27–29] to determine whether there is evidence for such turbulence.

The importance of changes in the poloidal flux in runaway physics was emphasized in [25]. The dual role of γ_{ef}, which is derived in this section, is new. It determines not only the poloidal flux change required for an e-fold in the number of runaway electrons but also the energy distribution of runaway electrons that result from an avalanche process. The efficiency of the transfer from poloidal field to relativistic electron energy and the number of runaway strikes to be expected in one disruption event will be shown to depend on γ_{ef}.

3.1. Remaining energetic electrons

The number of electrons with sufficient energy to runaway that remain after a thermal quench, called seed electrons, is difficult to reliably estimate.

The coefficient ϵ_f is defined so that when the source of the seed electrons is the tail of a Maxwellian and electrons with $\epsilon \equiv mv^2/2T > \epsilon_f$ can runaway, then there is a sufficient number of energetic electrons to carry the full current after acceleration to near the speed of light. The coefficient ϵ_f is given by

$$\mathcal{F}_{tail}^{(Max)}(\epsilon_f) = \frac{j_\parallel}{j_c}; \tag{47}$$

$$\epsilon_f \approx 9.5 \text{ for ITER}, \tag{48}$$

where $\mathcal{F}^{(\mathrm{Max})}_{\mathrm{tail}}(\epsilon)$ is given in equation (A.4) and $j_c \equiv \mathrm{enc}$. Equivalently, there are sufficient seed electrons to carry the full current when their fraction of all electrons is $j_\parallel/j_c \approx 2\times 10^{-4}$ in standard ITER operating scenarios.

As will be shown, when electrons with a kinetic energy $\epsilon > \epsilon_f$ can runaway, only a tiny change in the poloidal flux, equation (50), is required for a transfer of the current from thermal to relativistic carriers. Transfers with little change in poloidal flux were seen [30] on TFTR.

When the fraction of electrons that can runaway is smaller than $j_\parallel/j_c$ by a factor of $\mathrm{e}^{-\sigma_s}$, the number of e-folds required from the avalanche process [1, 2] is σ_s.

Two sources of seed electrons are eliminated when the critical energy for runaway K_r exceeds 20 keV: electrons emitted in tritium decay, which have a maximum energy of 18.6 keV, and cold electrons energized by a collision with a fusion alpha particle, which have a maximum energy of 1.9 keV, given by $4m/M_\alpha$ times the maximum energy of an alpha particle, 3.5 MeV. Neither source is important unless essentially all tail electrons from the previously hot Maxwellian are lost during the thermal quench. The electron density and atomic number of the ions required to raise K_r above 20 keV for loop voltages in the range of 500 V could be accurately obtained using existing codes [31, 32].

The importance of Compton scattering of cold electrons to energies above K_r by gamma rays emitted by radiative decays in the walls has not been quantified. The energy of the gamma ray must exceed the required kinetic energy for runaway, and potential sources drop the higher the required energy.

When all other sources are eliminated, it is the leftover tail of a hot Maxwellian that provides the seed, and this source requires the plasma be cooled faster than the tail electrons are slowed by collisions. In addition, the Maxwellian tail becomes exponentially small as $\epsilon_\mathrm{r} \equiv K_\mathrm{r}/T$ becomes large, equation (A.4).

Direct experimental limits on the number of energetic electrons remaining after a thermal quench is of particular importance.

3.2. Kinetic energy required for runaway

The minimum kinetic energy for runaway K_r is approximately inversely proportional to the loop voltage $V_\ell = 2\pi R E_\parallel$. Equation (A.1) implies

$$K_\mathrm{r} > \frac{mc^2}{2}\frac{V_\mathrm{ch}}{V_\ell}, \text{ when } V_\ell \gg V_\mathrm{ch}, \tag{49}$$

where $V_\mathrm{ch} \equiv 2\pi R E_\mathrm{ch} \approx 2.9n/(10^{20}/\mathrm{m}^3)\mathrm{V}$ in ITER. E_ch is the Connor–Hastie electric field, appendix A.1. For $V_\ell = 500\mathrm{V}$, the required kinetic energy for runaway when $n = 10^{20}/\mathrm{m}^3$ is $K_\mathrm{r} > 1.5$ keV.

The minimum energy for runaway can be significantly larger than implied by equation (49). Radiation adds additional drag forces and pitch angle scattering can prevent a close alignment of the electron velocity with the electric field.

Pitch-angle scattering is proportional to $1+Z$, where Z is the atomic number of the background ions [33, 34]. When pitch-angle scattering is large, newly energized electrons gain energy diffusively but lose energy by a steady Coulomb drag, which increases the minimum energy for runaway [2, 25]. The increase in K_r is roughly in proportion to $\sqrt{1+Z}$, a dependence that was given in [2] or can be obtained from balancing terms in the kinetic equation.

3.3. Flux and energy required for an e-fold

When the loop voltage V_ℓ is large compared to the voltage required to balance the collisional drag on relativistic electrons, large-angle collisions cause an exponentiation in the number of relativistic electrons [1, 2].

As shown in an appendix to [25], the acceleration of electrons is given by the change in the poloidal magnetic flux $\delta\psi_\mathrm{p}$ outside a surface that contains a fixed toroidal flux. The change in the poloidal flux required for an e-fold can be written as $\gamma_{ef}\psi_{pa}$, where the poloidal flux change required to accelerate a collisonless electron to a relativistic energy is

$$\psi_{pa} \equiv \frac{mc}{e}2\pi R \approx 0.0664 \text{ V} \cdot \text{ s} \tag{50}$$

in ITER. It is defined by $\delta(\gamma v_\parallel/c) = \delta\psi_\mathrm{p}/\psi_{pa}$, where $\gamma = 1/\sqrt{1-v^2/c^2}$. The flux change ψ_{pa} is about a thousand times smaller than the poloidal flux in ITER. The equation for the acceleration follows from $\mathrm{d}(\gamma m v_\parallel)/\mathrm{d}t = -eE_\parallel$ when the toroidal is large compared to the poloidal magnetic field. The parallel electric field $E_\parallel = -(\vec{B}/B)\cdot(\partial\vec{A}/\partial t)$, and $2\pi\vec{A} = -\psi_\mathrm{p}\vec{\nabla}\varphi + \psi_t\vec{\nabla}\theta$.

The dimensionless factor γ_{ef} will be discussed in sections 3.3.1 and 3.3.4 and is $2\ln\Lambda$ under idealized assumptions [2, 25]. In a cold plasma, $T = 100\,\mathrm{eV}$ and $n = 10^{20}/\mathrm{m}^3$, so $\gamma_{ef} = 2\ln\Lambda \sim 25$.

3.3.1. Energy and energy distribution of runaways. The factor γ_{ef} is closely related to the expected energy distribution of the relativistic electrons. This relationship is simple when the relativistic electrons are collisionlessly accelerated by a parallel electric field and their number N_r increases at a rate proportional to their number by the introduction of low energy electrons, which will be approximated as having zero momentum. The distribution function f can then be taken to be a delta function in pitch, which obeys the kinetic equation in momentum $p = \gamma mc$ space

$$\frac{\partial f}{\partial t} = eE_\parallel\frac{1}{p^2}\frac{\partial(p^2 f)}{\partial p} - N_\mathrm{r}\frac{\delta(p)}{p^2}\frac{\mathrm{d}\psi_\mathrm{p}/\mathrm{d}t}{\gamma_{ef}\psi_{pa}} \tag{51}$$

$$N_\mathrm{r} = \int f(p)p^2\mathrm{d}p \text{ so} \tag{52}$$

$$N_\mathrm{r} = N_\mathrm{r}(0)\exp\left(\left|\frac{\delta\psi_\mathrm{p}}{\gamma_{ef}\psi_{pa}}\right|\right). \tag{53}$$

This kinetic equation is solved by $p^2 f = g\left(p - e\int E_\parallel \mathrm{d}t\right)$, where $\int E_\parallel \mathrm{d}t = -\delta\psi_\mathrm{p}/2\pi R$. The function g can be obtained from the exponential dependence of N_r on $\delta\psi_\mathrm{p}/\gamma_{ef}\psi_{pa}$. The solution is

$$f = \frac{1}{p_0 p^2} N_\mathrm{r}(t)\mathrm{e}^{-p/p_0} \tag{54}$$

$$p_0 = \gamma_{ef} mc. \tag{55}$$

That is, the number of relativistic electrons drops exponentially as a function of γ, and $\bar{\gamma} \equiv \int \gamma f p^2 \mathrm{d}p / \int f p^2 \mathrm{d}p = \gamma_{ef}$.

The energy $(\gamma_{ef} - 1)mc^2$ is the kinetic energy an electron typically reaches before it knocks a cold electron up to an energy K_r at which it can run away. The energetic electron looses only a small fraction of its energy in the process. Any process that is important only for electrons with a $\gamma \gg \gamma_{ef}$ has only an exponentially small, $\sim \exp(-\gamma/\gamma_{ef})$, effect on the transfer of the current from thermal to relativistic carriers.

The energy W_r in relativistic electrons at any particular time is small compared to the energy contained in the poloidal magnetic field $W_p \approx 0.3 I_\mathrm{p}\Psi_\mathrm{p}$, section 2.4. W_r is the average kinetic energy per relativistic electron $(\bar{\gamma} - 1)mc^2$ times the number N_r of relativistic electrons. When the relativistic electrons carry a toroidal current I_r, the number is $N_\mathrm{r} = 2\pi R I_\mathrm{r}/ec$, so

$$W_\mathrm{r} = (\bar{\gamma} - 1) I_\mathrm{r} \psi_{pa}. \tag{56}$$

The energy taken from the poloidal magnetic field to accelerate electrons is $\delta W_p \approx 0.6 I_\mathrm{p}\delta\Psi_\mathrm{p}$, where $\delta\Psi_\mathrm{p} = -\sigma_s\gamma_{ef}\psi_{pa}$ and σ_s is the number of exponentiations required in the number of energetic electrons. The implication is that only $\approx 1/\sigma_s$ of the energy taken from the magnetic field is transferred to the relativistic electrons. The rest is dissipated by the resistivity of the near-thermal current carriers.

3.3.2. Maximum number of e-folds. The poloidal flux in the ITER plasma is $\Psi_\mathrm{p} \approx 80\ \mathrm{V}\cdot\mathrm{s}$, so the maximum number of e-folds in the number of energetic electrons is

$$\sigma_\mathrm{max} = \frac{1}{\gamma_{ef}}\frac{\Psi_\mathrm{p}}{\psi_{pa}}, \tag{57}$$

which for $\gamma_{ef} = 25$ makes $\sigma_\mathrm{max} \approx 40$.

The largest $\epsilon \equiv mv^2/2T$ of interest for transfer of the current to relativistic carriers using tail electrons from the Maxwellian is either

$$\epsilon_\mathrm{max} = \epsilon_f + \sigma_\mathrm{max}, \tag{58}$$

or $\epsilon_\mathrm{max} \approx 53$ set by the condition that there be at least one tail electron with such a high energy, whichever is smaller. The coefficient ϵ_f is the coefficient for a fast transfer, equation (47).

When there are sufficient electrons from the pre-thermal-quench hot Maxwellian that survive and are above the critical energy for runaway to carry the full plasma current, then the runaway is fast since a poloidal flux change of only ψ_{pa} is required, which in ITER would occur about a thousand times faster than the $L/\mathcal{R}$ time for the current. The $L/\mathcal{R}$ time itself must be less than about 150ms to remove the poloidal flux before the plasma drifts into the wall.

3.3.3. Multiple runaway strikes. When the kinetic energy required for runaway satisfies $\epsilon \ll \epsilon_\mathrm{max}$, only a small fraction of the poloidal flux in the plasma is consumed in transferring the current to relativistic electrons. If most but not all of the initial group of relativistic electrons are lost—for example because the current profile becomes tearing unstable—the short term effect is to transfer the current back to thermal carriers. The relativistic current can then rebuild itself from the remaining relativistic electrons. For example if ninety percent of the relativistic electrons are lost, 2.3 e-folds in the number of energetic electrons can restore the relativistic current. That is the walls can undergo multiple relativistic electron strikes as the poloidal flux is removed.

Putvinski *et al* [35] envisioned a surface current of runaway electrons forming just inside the body of a plasma as the plasma drifts towards the wall. Continual rejuvenation of this surface current would allow a large fraction of the poloidal magnetic energy to be carried to the walls by relativistic electrons. This process need not occur. A drift need not change the poloidal flux as a function of the toroidal flux $\psi_\mathrm{p}(\psi_t)$ in the body of the plasma, and this function must change to accelerate electrons. At the plasma edge, $\psi_\mathrm{p}(\psi_t)$ involves the change in the external poloidal flux since the drift into the wall is on the time scale of flux penetration through the walls.

Martín-Solís *et al* [36] have an extensive discussion of the fraction of the energy in the poloidal magnetic field that can be transferred to the walls by relativistic electrons using a zero-dimensional model of runaway electron losses, effectively a diffusive-loss model.

3.3.4. Calculations of γ_{ef}. The larger γ_{ef} the weaker the avalanche effect since $\sigma_\mathrm{max} \propto 1/\gamma_{ef}$. Possibly the most important contribution that theory and simulation could quickly make is a far more reliable determination γ_{ef} for any given state of the ITER plasma.

In the standard model of the avalanche [2], the rate electrons are brought above the critical energy for runaway K_r is inversely proportional to K_r. The implication is that γ_{ef} should be approximately proportional to $\sqrt{1+Z}$. Existing codes [31, 32] could give a more accurate answer, but the standard model for the avalanche requires modification for reliable answers to be obtained [25].

4. Discussion

For ITER to address its mission, a strategy must be devised so major incidents involving relativistic electrons occur less than once in a thousand shots. Thermal quenches give conditions conducive to the transfer of the plasma current from near thermal to relativistic electron carriers. In devising a strategy to avoid this transfer and in using data from existing tokamaks to provide evidence for the effectiveness, two pairs of concepts are of central importance:

1. Destruction versus preservation of magnetic surfaces during thermal quenches.
   (a) Magnetic surfaces appear to be destroyed within $\sim$ 1ms, over much of the plasma volume during a thermal quench.
   (b) Electrons can be accelerated to relativistic energies only in flux tubes in which the magnetic field lines remain confined and some surfaces persist.
2. Quasi-ideal versus resistive evolution during and shortly after a thermal quench.
   (a) A quasi-ideal evolution is consistent with the destruction of magnetic surfaces on an Alfvénic time scale.
   (b) A resistive evolution is required to accelerate electrons to relativistic energies.

The interpretation and extrapolation of data from existing tokamaks to ITER should be consistent with these two pairs of concepts. Unfortunately, the separation of a quasi-ideal from a resistive evolution in large tokamaks at high temperatures requires the resolution of spatial scales much smaller than those in existing simulations using the non-linear codes NIMROD [37], JOREK [38], M3D [39], and M3D-C1 [40]. In addition, interpretation and extrapolation require the study of many cases, so the computer resources devoted to each study must be limited.

Fortunately, Maxwell's equations place strong constraints on what is possible during a quasi-ideal evolution, section 2.3.1: magnetic helicity is conserved and electrons receive no direct acceleration. In section 2 this paper derives the quasi-ideal constraints and in section 3 places the resistive evolution in the flux tubes of confined field lines into a form in which the central issues in electron runaway can be assessed. Representative applications of these equations to the interpretation of existing experiments will be in a future paper, where it will be shown how the [41] helicity conserving, mean-field expression $\vec{E}\cdot\vec{B} = -\vec{\nabla}\cdot\{\lambda\vec{\nabla}(j_\parallel/B)\}$ can be used in rapid studies of the implications of the two pairs of concepts. Within the plasma volume mean-field theory approximates the flux of poloidal magnetic flux, $\mathcal{F}_\parallel$, equation (11), by a flux $\mathcal{F}_{\rm mf}$, which is linearly proportional to $\partial^2 I/\partial\psi_t^2$. The ratio of $\mathcal{R}_\psi$, equation (20), and λ determines the ratio of resistive to quasi-ideal evolution.

Rapid thermal quenches can occur either naturally [13] or during mitigated disruptions [14, 15]. In simulations of experiments, rapid thermal quenches are associated with fast magnetic reconnections, which break the magnetic surfaces over much of the plasma volume causing a rapid flattening of the $j_\parallel/B$ profile, a large reduction in the internal inductance ℓ_i, and an upward spike in the plasma current on a 1 ms time scale. Electrons cannot reach a relativistic energy in plasma regions in which the field lines strike the walls in less that roughly a thousand toroidal circuits, and far more circuits are required for even one e-fold in the number of electrons by the avalanche mechanism [1, 2], a factor $\gamma_{ef}\sim 2\ln\Lambda\sim 25$ more.

The poloidal flux change required to increase the kinetic energy of electrons by mc^2 is $\psi_{pa} = 2\pi R_0 mc/e \approx 0.0664\,\mathrm{V}\cdot\mathrm{s}$. The poloidal flux change required for an e-fold in the number of energetic electrons by the avalanche mechanism is $\gamma_{ef}\psi_{pa}$. The rate at which a single collision can increase the kinetic energy of an electron from negligible to the energy required for runaway $K_{\rm r}$ has no direct dependence on $\ln\Lambda$ but is inversely dependent on $K_{\rm r}$. $K_{\rm r}$ is proportional $\ln\Lambda$, so γ_{ef} is proportional to $\ln\Lambda$. The kinetic energy required for runaway becomes larger with the atomic number Z of the background ions, whether fully ionized or not, and when $K_{\rm r} > 18.6$ keV tritium decay cannot provide seed electrons. Improved calculations of γ_{ef} might significantly increase its value, in part through an increased $K_{\rm r}$, but also because the standard theory [1, 2] is an approximation [25].

Although γ_{ef} is only implicitly discussed in the existing literature, it defines not only the poloidal flux change required for an e-fold, $\gamma_{ef}\psi_{pa}$, but also the energy distribution of runaway electrons that is obtained from an avalanche. The average electron energy obtained from an avalanche is $\gamma_{ef}mc^2$. An increase in γ_{ef} above its expected value proportionately reduces the maximum number of avalanche e-folds possible in ITER but proportionately increases the energy of the electrons in a relativistic current. Any effects that arise at energies large compared to $\gamma_{ef}mc^2$ have little practical effect on the dangers of runaway electrons. Factors of two in γ_{ef} are important.

The poloidal flux outside of a magnetic surface that contains a given toroidal flux can change on the time scale for $j_\parallel/B$ to flatten, but the helicity content K_c and hence the bulk of the poloidal flux require a resistive time scale to be quenched. It is the removal of the bulk of the poloidal flux on the resistive wall time that is required to avoid a halo current.

When not all of the magnetic surfaces are broken, a skin current is induced on the surface of the flux tubes that contain field lines that do not intercept the chamber walls. When the poloidal flux change expected from the resistive relaxation of the skin current is sufficiently large and rapid, one would expect hot tail electrons to be accelerated to high energies. Their existence and location would be a clear diagnostic of the existence and extent of non-intercepting flux tubes, but such measurements must be sensitive to an energetic-electron density of order j/ec to provide evidence that relativistic electrons do not exist. When there is a sufficient number of electrons above the runaway energy to carry the full current density without the need for e-folding, Aleynikov and Breizman [42] have found that the current-carrying electrons may reach energies of only 100's of keV before the acceleration saturates. Saturation occurs when the current is being carried by energetic rather than near thermal electrons, which implies the density of energetic, near relativistic, electrons must be $\approx j/ec$. A diagnostic may be needed that can show that electrons of 100's of keV of density j/ec do not exist.

The simplest diagnostic for the breakup of magnetic surfaces is the upward spike in the current. Unfortunately, an empirical study of the parametric dependence of the magnitude and time scale of the current spikes associated with tokamak current quenches has not been published, which is indicative that the importance of current spikes and the period of magnetic surface breakup have not been fully appreciated.

The time scale observed for upward spikes ~ 1 ms and the time of a few microseconds for an Alfvén wave to encircle a tokamak toroidally imply a few hundred transits are required for a magnetic field line to cover the reconnected region, this number of transits is consistent with the relaxation of the electron temperature, appendix A.2.2.

Whatever the strategy may be for avoiding large currents of relativistic electrons, it would be desirable to also have a strategy for dissipating such currents other than by a destructive wall interception. The transfer of the current from thermal to relativistic carriers can be fast and can require a poloidal flux change as small as $\psi_{pa} \approx 0.066$ V· s in ITER, section 3.3. Indeed, very fast transfers with an indeterminately small change in poloidal flux were seen [30] in TFTR. The vertical-field system in ITER is thought to be inadequate for maintaining axisymmetric position control of a runaway current [43], so the dissipation of relativistic currents in ITER must apparently be on the time scale for the plasma to drift due to wall resistivity, ~ 150 ms. Even if the vertical-field system were adequate, the plasma current carried by relativistic electrons must be quenched without exciting tearing modes or kinks, which can throw the relativistic electrons into the walls. Increasing the plasma density by impurity injection is likely to produce a large scale breakup of magnetic surfaces when the impurities reach the $q = 2$ surface. This is seen in simulations of massive gas and shattered pellet injection [5–7] into plasmas in which the current is carried by near-thermal electrons. Because the growth rate of tearing modes is determined by near-thermal electrons [44], little difference is expected in the conditions or speed of surface breakup depending on whether the current carriers are near-thermal or relativistic electrons though a relativistic-electron current evolves towards regions of low density rather high temperature.

DIII-D experiments have shown a benign termination of plasmas with relativistic electron currents [45], but these had relativistic electron currents $\lesssim 400$ kA, approximately a third of the current that had been carried by near thermal electrons. The large edge safety factor $q_e \gtrsim 10$ makes these experiments far more stable to tearing and kink instabilities than plasmas with a lower q_e. Runaway electron currents in ITER may arise that have a much lower safety factor; the presence of a $q = 2$ surface appears important [5–7]. In any case, the density must be raised at the plasma center to rapidly dissipate the current density of relativistic electrons there, whether the density increase is due to direct injection, diffusion, or mixing.

Although present ITER planning for disruption mitigation revolves around issues of magnetic surface breakup, the success of this strategy is not clear. The use of impurity injection and associated surface breakup to avoid halo and runaway-electron currents requires that non-intercepting flux tubes be dissipated before outer magnetic surfaces re-form—otherwise a strong relativistic electron current will be driven and a particularly dangerous situation can arise in which a large number of relativistic electrons can be released in a short pulse along a narrow flux tube [20]. The use of impurity injection to speed relativistic current dissipation requires that the magnetic field lines that confine the relativistic electrons must not be allowed to strike the walls either through tearing or kinking. In principle, appendix A.1, the plasma current in ITER could be terminated over the full range of acceptable times, roughly 50 to 150 ms, by cooling with no danger of producing relativistic runaways. But, this requires a carefully orchestrated strategy for cooling, which preserves magnetic surfaces. If natural thermal quenches can be avoided by preemptive plasma termination as suggested by [13], then surface-preserving plasma cooling could be the primary strategy for avoiding damaging relativistic electrons.

A central issue in devising strategies for the avoidance of runaway electrons is whether the plasma current can be quenched orders of magnitude faster than the initial current-quench time without breaking magnetic surfaces or driving external kinks. This is in principle possible when the electron temperature as a function or radius and time, $T(r, t)$, can be sufficiently accurately controlled that the plasma current can be reduced while holding the current in a stable profile. If adequate control is feasible, relativistic electrons could be safely avoided by plasma cooling. If adequate density control is feasible, $n(r, t)$, relativistic electron beams could be dissipated by increasing the background electron density while maintaining a stable current profile.

Acknowledgment

This material is based upon work supported by the U.S. Department of Energy, Office of Science, Office of Fusion Energy Sciences under Award No. DE-FG02-03ER54696 and DE-SC0016347.

Appendix. Plasma cooling

A.1. Absence of a Maxwellian runaway

This section will show that for sufficiently slow cooling, $\gtrsim 23$ ms, a significant runaway cannot occur until the temperature is below a few electron Volts. This temperature is below the lowest temperature consistent with a tolerable time for the current quench in ITER. The required cooling to obtain a runaway is far faster than the rate ITER plasmas can drift into the walls.

The drag force of background electrons of density n on an energetic electron with momentum $p = \gamma mv$ is $\mathrm{d}p/\mathrm{d}t = -eE_{\mathrm{ch}}c^2/v^2$, where the Connor–Hastie electric field [46] is $E_{\mathrm{ch}} = ne^3 \ln(\Lambda)/(4\pi\epsilon_0^2 m_e c^2)$. For runaway, the acceleration of electrons along the magnetic field by the electric field must exceed the collisional drag,

$$\left|eE_{\|}\right| > \left|eE_{\mathrm{ch}}c^2/v^2\right|. \tag{A.1}$$

The Ohmic electric field provides the acceleration, $E_{\|} = \eta j_{\|}$ with η the Spitzer resistivity, which can be written as

$$E_{\|} = \frac{2}{3}\frac{0.51}{\sqrt{2\pi}}E_{\mathrm{ch}}\left(\frac{mc^2}{T}\right)^{3/2}\frac{j_{\|}}{j_c}, \text{ where} \tag{A.2}$$

$$j_c \equiv \mathrm{enc} \approx 4.80 \times 10^3 \frac{n}{10^{20}/\mathrm{m}^3}\frac{\mathrm{MA}}{\mathrm{m}^2}. \tag{A.3}$$

When $\epsilon \equiv mv^2/2T \gg 1$, the fraction of the electrons in a non-relativistic Maxwellian that are at a higher energy than $mv^2/2$ is

$$\mathcal{F}_{\rm tail}^{\rm (Max)}(\epsilon) = \frac{2\sqrt{\epsilon}}{\sqrt{\pi}} {\rm e}^{-\epsilon}. \tag{A.4}$$

The coefficient $\epsilon_{\rm max}$ is defined so that when $\epsilon > \epsilon_{\rm max}$, there are too few electrons for a significant runaway. For example, at the standard ITER operating density of $10^{20}/{\rm m}^3$ there are $\sim 10^{22} \sim e^{50}$ electrons in ITER. Not even one electron is expected when $\epsilon \gtrsim 53$. As will be shown below, $\epsilon_{\rm max} \lesssim 50$.

The requirement that there be a sufficiently strong ohmic electric field to accelerate electrons with a kinetic energy with $\epsilon < \epsilon_{\rm max}$ implies

$$\left| \frac{eE_{\rm ch} mc^2}{2\epsilon_{\rm max} T} \right| < \left| eE_\| \right|, \text{ or} \tag{A.5}$$

$$T < \epsilon_{\rm max}^2 \left(\frac{4}{3} \frac{0.51}{\sqrt{2\pi}} \right)^2 \left(\frac{j_\|}{j_c} \right)^2 mc^2 \tag{A.6}$$

The current density in ITER is $j_\| \sim 1\,{\rm MA\ m}^{-2}$, which implies $j_\|/j_c \sim 2 \times 10^{-4}$, so $T \lesssim 1.5 \times 10^{-3} \epsilon_{\rm max}^2$ eV for runaway. When $\epsilon_{\rm max} = 50$, runaway can occur when $T \lesssim 4$ eV.

In order for the cooling to maintain a Maxwellian distribution, the cooling must be slow compared to the thermalization time $\tau_{\rm th}$ of the most energetic particles that are relevant to the runaway process, which means particles with an energy $\epsilon_{\rm max} T$.

The time $\tau_{\rm th}$ is determined by how long the equation ${\rm d}p/{\rm d}t = -eE_{\rm ch} c^2/v^2$ predicts is required for p to go to zero. Since $c^2/v^2 = 1 + (mc/p)^2$, the thermalization time has two simple limits. When the initial momentum satisfies $p_0/mc = \gamma_0 \gg 1$, the thermalization time $\tau_{\rm th} = \gamma_0/\nu_{\rm ch}$, and when $p_0/mc \ll 1$, the thermalization time $\tau_{\rm th} = (\nu_0/c)^3/(3\nu_{\rm ch})$, where

$$\nu_{\rm ch} \equiv \frac{eE_{\rm ch}}{mc} \approx \frac{1}{22.7{\rm ms}} \frac{n}{10^{20}/{\rm m}^3};. \tag{A.7}$$

When $\epsilon_{\rm max} T \ll mc^2$, the thermalization time is $\tau_{\rm th} = (2^{3/2}/3)(\epsilon_{\rm max} T/mc^2)^{3/2}/\nu_{\rm ch}$.

A.2. Methods of plasma cooling

This section reviews the three possible cooling methods: (1) cross-surface transport, (2) magnetic surface breakup, and (3) radiation cooling. A rapid quench of the plasma current, $\lesssim 150$ ms, requires strong plasma cooling.

A.2.1. Cooling by cross-surface transport. Thermal transport across the magnetic surfaces appears inadequate to provide cooling on the required time scale.

A limit on cross-surface transport is given by Bohm diffusion. The variation in the electric potential within a magnetic surface is constrained by quasi-neutrality, which implies $\delta\Phi \lesssim T/e$. When b and a are the two radii of an elliptical surface this implies the time required for particles to $E \times B$ drift across the plasma is $\tau_{\rm Bohm} \sim \pi ab/(\pi T/eB)$. Now $\pi T/eB \sim 6(T/10\,{\rm keV})\ {\rm m^2 ms^{-1}}$ when $B = 5.3$ T. The cross-sectional area of ITER is $S_* \sim 22\ {\rm m}^2$, so $\tau_{\rm Bohm} \sim 4(10\,{\rm keV}/T)$ ms, which is slow compared to the thermal quench, ~ 1 ms. The slowness of Bohm diffusion also limits the speed with which impurities can be transported into the plasma core by turbulent fluctuations in the electric potential.

A.2.2. Cooling by magnetic surface breakup. Magnetic field lines deep in the plasma volume can intercept the walls when the magnetic surfaces are broken. Thermal conduction along the field lines that make N_t toroidal transits between interceptions with the walls can give a very rapid rate of loss of electron energy $\nu_{\rm cool}$. Using the Braginskii's expression [47] for the parallel electron conductivity, $\kappa_\| \approx 3.16 nT_e/m\nu_c$, and assuming a temperature profile proportional to $\sin(\pi z/L)$, where z is the coordinate along magnetic field lines of length $L = 2\pi R N_t$,

$$\begin{aligned} \nu_{\rm cool} &\approx 3.2 \left(\frac{\pi}{2\pi R N_t} \right)^2 \frac{T}{m\nu_c} \\ &\approx \frac{10^{10}}{N_t^2} \left(\frac{T}{10\,{\rm keV}} \right)^{5/2} \left(\frac{10^{20}/{\rm m}^3}{n} \right) \frac{1}{\rm s}, \end{aligned} \tag{A.8}$$

$$\nu_c \approx 4.5 \times 10^3 \left(\frac{10\,{\rm keV}}{T} \right)^{3/2} \left(\frac{n}{10^{20}/{\rm m}^3} \right) \frac{1}{\rm s}, \tag{A.9}$$

where ν_c is the electron collision frequency. The formula is valid only when $\nu_c > \nu_{\rm cool}$. At standard ITER conditions of $T = 10$keV and $n = 10^{20}/{\rm m}^3$, it takes $N_t \approx 2000$ transits for the cooling time to be longer than the collision time of $\approx$0.2 ms. As discussed, the time scale of the current spike, ~ 1 ms, implies $N_t \sim 300$. The cooling rate becomes slower than 1/ms with $N_t = 300$ when T drops below 400 eV. Further cooling requires longer times or radiation. The different behavior of natural current quenches in JET after the change to metal walls is thought to be due to the reduction in radiating impurities [13].

A.2.3. Cooling by radiation. Radiative cooling can in principle be controlled by an appropriate impurity injection. If cooling were adequately controlled, an ITER plasma could be quickly shutdown without runaways by keeping the electron distribution close to a Maxwellian and maintaining magnetic surfaces.

Controlled cooling by radiation is difficult for three reasons. (1) The rate of cooling for a given quantity of impurity can increase faster than the Coulomb collision frequency as the temperature of the plasma is reduced. The implication is that the cooling can become so fast that electrons in the energetic tail can separate from the Mawellian and runaway as the plasma is cooled. This issue might be addressed by using a mixture of impurities that have different radiation curves, and studies should be done on whether suitable mixtures exist. (2) The radial profile of the cooling is important. Without central impurity injection, it is difficult to cool the central plasma on a appropriate time scale. In addition, a changing temperature profile causes the current profile to change, which can result in kink and tearing instabilities. (3) Even if appropriate

impurity injection strategies are identified, a method of delivering the impurities with the required temporal and spatial profiles requires development. Massive-gas injection and shattered pellets are unlikely to offer sufficient control.

References

[1] Jayakumar R., Fleischmann H.H. and Zweben S.J. 1993 *Phys. Lett.* A **172** 447
[2] Rosenbluth M.N. and Putvinski S.V. 1997 *Nucl. Fusion* **37** 1355
[3] Hender T.C. *et al*, The ITPA HD, Disruption and Magnetic Control Topical Group 2007 *Nucl. Fusion* **47** S128
[4] Lehnen M. *et al* and EFDA JET contributors 2015 *J. Nucl. Mater.* **463** 39
[5] Izzo V.A. *et al* 2011 *Nucl. Fusion* **51** 063032
[6] Izzo V.A., Humphreys D.A. and Kornbluth M. 2012 *Plasma Phys. Control. Fusion* **54** 095002
[7] Fil A. *et al* and JET Contributors 2015 *Phys. Plasmas* **22** 062509
[8] Nardon E., Fil A., Hoelzl M., Huijsmans G. and JET contributors 2017 *Plasma Phys. Control. Fusion* **59** 014006
[9] Loureiro N.F. and Uzdensky D.A. 2016 *Plasma Phys. Control. Fusion* **58** 014021
[10] Boozer A.H. 2014 *Phys. Plasmas* **21** 072907
[11] Boozer A.H. 2015 *Nucl. Fusion* **55** 025001
[12] Similon P.L. and Sudan R.N. 1989 *Astrophys. J.* **336** 442
[13] de Vries P.C. *et al*, The COMPASS Team, The ASDEX Upgrade Team and JET Contributors 2016 *Nucl. Fusion* **56** 026007
[14] Lehnen M., Gerasimov S.N., Jachmich S., Koslowski H.R., Kruezi U., Matthews G.F., Mlynar J., Reux C., de Vries P.C. and JET contributors 2015 *Nucl. Fusion* **55** 123027
[15] Shiraki D., Commaux N., Baylor L.R., Eidietis N.W., Hollmann E.M., Lasnier C.J. and Moyer R.A. 2016 *Phys. Plasmas* **23** 062516
[16] Boozer A.H. 2015 *Phys. Plasmas* **22** 102511
[17] Papp G., Drevlak M., Pokol G.I. and Fülöp T. 2015 *J. Plas. Phys.* **81** 475810503
[18] Abdullaev S.S., Finken K.H., Wongrach K. and Willi O. 2016 Theoretical and experimental studies of runaway electrons in the TEXTOR tokamak *Schriften des Forschungszentrums Jülich Reihe Energie & Umwelt / Energy & Environment, Band / Volume* vol 318 (Jülich: Forschungszentrum Jülich GmbH Zentralbibliothek)
[19] Boozer A.H. 2016 *Phys. Plasmas* **23** 082514
[20] Boozer A.H. and Punjabi A. 2016 *Phys. Plasmas* **23** 102513
[21] Taylor J.B. 1974 *Phys. Rev. Lett.* **33** 1139
[22] Boozer A.H. 2011 *Plasma Phys. Control. Fusion* **53** 084002
[23] Smith H.M., Boozer A.H. and Helander P. 2013 *Phys. Plasmas* **20** 072505
[24] Woltjer L. 1958 *Proc. Natl Acad. Sci. USA* **44** 489
[25] Boozer A.H. 2015 *Phys. Plasmas* **22** 032504
[26] Liu C., Brennan D.P., Boozer A.H. and Bhattacharjee A. 2017 *Plasma Phys. Control. Fusion* **59** 24003
[27] Granetz R.S., Esposito B., Kim J.H., Koslowski R., Lehnen M., Martin-Solis J.R., Paz-Soldan C., Rhee T., Wesley J.C., Zeng L. and the ITPA MHD Group 2014 *Phys. Plasmas* **21** 072506
[28] Paz-Soldan C. *et al* 2014 *Phys. Plasmas* **21** 022514
[29] Reux C. *et al* and JET contributors 2015 *Nucl. Fusion* **55** 093013
[30] Fredrickson E.D., Bell M.G., Taylor G. and Medley S.S. 2015 *Nucl. Fusion* **55** 013006
[31] Stahl A., Hirvijoki E., Decker J., Embreus O. and Fülöp T. 2015 *Phys. Rev. Lett.* **114** 115002
[32] Liu C., Brennan D.P., Bhattacharjee A. and Boozer A.H. 2016 *Phys. Plasmas* **23** 010702
[33] Beliaev S.T. and Budker G.I. 1956 *Sov. Phys.—Dokl.* **1** 218
[34] Karney C.F.F. and Fisch N.J. 1985 *Phys. Fluids* **28** 116
[35] Putvinski S., Barabaschi P., Fujisawa N., Putvinskaya N., Rosenbluth M.N. and Wesley J. 1997 *Plasma Phys. Control. Fusion* **39** B157
[36] Martín-Solís J.R., Loarte A., Hollmann E.M., Esposito B., Riccardo V., FTU and DIII-D Teams and JET EFDA Contributors 2014 *Nucl. Fusion* **54** 083027
[37] Glasser A.H., Sovinec C.R., Nebel R.A., Gianakon T.A., Plimpton S.J., Chu M.S., Schnack D.D. and The NIMROD Team 1999 *Plasma Phys. Control. Fusion* **41** A747
[38] Huysmans G. 2005 *Plasma Phys. Control. Fusion* **47** 2107
[39] Park W., Belova E.V., Fu G.Y., Tang X.Z., Strauss H.R. and Sugiyama L.E. 1999 *Phys. Plasmas* **6** 1796
[40] Breslau J., Ferraro N. and Jardin S. 2009 *Phys. Plasmas* **16** 092503
[41] Boozer A.H. 1986 *J. Plasma Phys.* **35** 133
[42] Aleynikov P. and Breizman B.N. 2017 Generation of runaway electrons during the thermal quench in tokamaks *Nucl. Fusion* **57** 046009
[43] Gribov Y., Kavin A., Lukash V., Khayrutdinov R., Huijsmans G.T.A, Loarte A., Snipes J.A. and Zabeo L. 2015 *Nucl. Fusion* **55** 073021
[44] Helander P., Grasso D., Hastie R.J. and Perona A. 2007 *Phys. Plasmas* **14** 122102
[45] Hollmann E.M. *et al* 2013 *Nucl. Fusion* **53** 083004
[46] Connor J.W. and Hastie R.J. 1975 *Nucl. Fusion* **15** 415
[47] Braginskii S.I. 1965 *Rev. Plasma Phys.* **1** 205